Published October 5, 1998

Small Espin: A Third Actin-bundling Protein and Potential Forked Protein Ortholog in Brush Border Microvilli

James R. Bartles, Lili Zheng, Anli Li, Allison Wierda, and Bin Chen

Department of Cell and Molecular Biology, Northwestern University Medical School, Chicago, Illinois 60611

Abstract. An ~30-kD isoform of the actin-binding/bundling protein espin has been discovered in the brush borders of absorptive epithelial cells in rat intestine and kidney. Small espin is identical in sequence to the COOH terminus of the larger (~110-kD) espin isoform identified in the actin bundles of Sertoli cell–spermatid junctional plaques (Bartles, J.R., A. Wierda, and L. Zheng. 1996. *J. Cell Sci.* 109:1229–1239), but it contains two unique peptides at its NH_2 terminus. Small espin was localized to the parallel actin bundles of brush border microvilli, resisted extraction with Triton X-100, and accumulated in the brush border during enterocyte differentiation/migration along the crypt–villus axis in adults. In transfected BHK fibroblasts, green fluorescent protein–small espin decorated F-actin–containing fibers and appeared to elicit their accumulation and/or bundling. Recombinant small espin bound to skeletal muscle and nonmuscle F-actin with high affinity (K_d = 150 and 50 nM) and cross-linked the filaments into bundles. Sedimentation, gel filtration, and circular dichroism analyses suggested that recombinant small espin was a monomer with an asymmetrical shape and a high percentage of α-helix. Deletion mutagenesis suggested that small espin contained two actin-binding sites in its COOH-terminal 116–amino acid peptide and that the NH_2-terminal half of its forked homology peptide was necessary for bundling activity.

Key words: cytoskeleton • actins • microvilli • intestines • kidney

The ability of actin to form filaments and higher-order cross-linked structures is harnessed by cells in a variety of ways to make the cortical actin cytoskeleton a central determinant of cellular shape, division, motility, adhesion, and signaling. These feats are accomplished in large part through the activities of a host of different actin-binding proteins, which among other things: (*a*) regulate the polymerization and depolymerization of actin; (*b*) connect actin-based structures to membranes or other cytoskeletal systems; (*c*) power movement relative to actin filaments; or (*d*) cross-link F-actin into meshworks or bundles (Pollard, 1993; Ridley, 1995; Burridge and Chrzanowska-Wodnicka, 1996; Gumbiner, 1996; Mitchison and Cramer, 1996; Bretscher et al., 1997; Carlier, 1997; Hall, 1998; Mermall et al., 1998).

Actin bundles can be either of mixed polarity (contractile bundles) or of uniform polarity (parallel bundles) (Matsudaira, 1991; Pollard, 1993; Furukawa and Fechheimer, 1997). Parallel bundles are commonly associated with relatively long-lived specializations of the cell surface, where they appear to function in part as a scaffold to support evaginations or invaginations of the plasma membrane. Examples include: the brush border microvilli of absorptive epithelia (Heintzelman and Mooseker, 1992; Fath and Burgess, 1995), the stereocilia of hair cells in the inner ear (Tilney et al., 1992), the bristles of *Drosophila* pupae (Tilney et al., 1995), and the submembranous plaques of Sertoli cell–spermatid and Sertoli cell–Sertoli cell junctions known as ectoplasmic specializations (Russell and Peterson, 1985; Vogl, 1989; Bartles et al., 1996). There is evidence that each of these structures contains its own complement of actin-bundling proteins. In three of these cases, the structure in question is known to contain at least two actin-bundling proteins that appear to function sequentially during the process of assembly: in brush border microvilli, villin and fimbrin/plastin (Rodman et al., 1986; Ezzell et al., 1989; Heintzelman and Mooseker, 1992; Fath and Burgess, 1995); in hair cell stereocilia, some yet-to-be identified protein (not villin) and fimbrin/plastin (Tilney et al., 1992); and in the bristles of *Drosophila* pupae, the proteins encoded by the *forked* and *singed* genes (the latter a fascin ortholog) (Tilney et al., 1995).

Actin cross-linking proteins typically display a modular organization (Matsudaira, 1991; Pollard, 1993; Puius et al., 1998). The ability to cross-link actin filaments requires that a protein contain two or more actin-binding sites per monomer or that it exist as a dimer or higher oligomer.

Address all correspondence to James R. Bartles, Department of Cell and Molecular Biology, Northwestern University Medical School, 303 East Chicago Avenue, Chicago, IL 60611. Tel.: (312) 503-1545. Fax: (312) 503-7912. E-mail: j-bartles@nwu.edu

Published October 5, 1998

The spacing between the actin-binding sites appears to influence the type of cross-linked structure formed. Proteins that cross-link actin filaments to form loose meshworks are typically larger and achieve relatively distant separations between their actin-binding sites through the use of extended spacer peptides and/or through the formation of dimers or higher oligomers. In contrast, proteins that cross-link filaments into bundles are generally smaller in size and have tandem actin-binding sites spaced relatively close together. For example, the known actin-bundling proteins of brush border microvilli, fimbrin/plastin and villin, are both monomeric and contain tandem actin-binding sites. Fimbrin/plastin contains two tandemly repeated 27-kD actin-binding domains of the α-actinin/β-spectrin type, each of which in turn is composed of two calponin-homology domains (Matsudaira, 1991; Goldsmith et al., 1997). Villin contains a "core" domain, which displays Ca^{2+}-mediated F-actin severing activity and is made up of six repeats of a domain shared with other severing proteins (such as gelsolin, fragmin, and severin) and a unique thermostable COOH-terminal "headpiece," which is required for actin-bundling activity (Friederich et al., 1990; McKnight et al., 1996, 1997). In addition to containing modules for binding to actin, actin-bundling proteins frequently contain other modules that can regulate bundling activity. For example, both fimbrin and villin contain binding sites for Ca^{2+}, and the actin-bundling activity of both proteins is decreased dramatically by physiological concentrations of Ca^{2+} (Glenney et al., 1981; Alicea and Mooseker, 1988; Namba et al., 1992; Lin et al., 1994). In fact, villin becomes an F-actin–severing protein in the presence of Ca^{2+} (Walsh et al., 1984).

We recently identified espin as a novel ~110-kD actin-binding protein localized to the parallel actin bundles in the junctional plaque of Sertoli cell ectoplasmic specializations (Bartles et al., 1996). Upon sequence analysis, espin was found to contain eight ankyrin-like repeats in its NH_2-terminal third, a potential P-loop, two proline-rich peptides, and two peptides that contained clusters of multiple glutamates bracketed by arginines, lysines, and glutamines in a pattern reminiscent of the repetitive motif found in the protein trichohyalin. The ankyrin-like repeats and a 66–amino acid peptide present near the COOH terminus of espin showed 35–39% sequence identity to proteins encoded by the *forked* gene of *Drosophila.* A maltose-binding protein fusion protein containing the COOH-terminal 379 amino acids of espin was found to bind with high affinity to F-actin in vitro. And, when expressed by transfected NRK fibroblasts, the same COOH-terminal fragment of espin was observed to decorate actin fibers or cables and appeared to bring about their accumulation and/or bundling. On the basis of its structure, localization, and properties, we hypothesized that espin was involved in linking actin filaments to each other and/or to membranes, thereby potentially playing a key role in the organization and function of the ectoplasmic junctional specializations of Sertoli cells.

The ~110-kD espin of Sertoli cell ectoplasmic specializations was found to be encoded by an ~2.9-kb mRNA that, on Northern blots of total RNA, appeared specific to testis among 11 rat tissues examined (Bartles et al., 1996). At that time, we also detected crosshybridizing mRNAs of ~1.7 kb in rat small intestine and kidney. Here we report that the ~1.7-kb crosshybridizing mRNAs encode a second member of the espin family, a smaller isoform that displays a number of the properties expected for a newly identified actin-bundling protein of brush border microvilli.

Materials and Methods

Homogenates (~4%, wt/vol) were prepared from the testis, kidney, and small intestinal mucosal scrapings of adult rats in 0.25 M sucrose, 3 mM imidazole-HCl, pH 7.4, containing protease inhibitors (1 mM PMSF, 1 μg/ml each of antipain and leupeptin, and 10–20 TIU/liter of aprotinin) using eight up-and-down strokes of a motor-driven Teflon-glass homogenizer (3,000 rpm). Brush borders were isolated from the small intestines of adult rats in the presence of the protease inhibitors using the procedure of Keller and Mooseker (1982). In some experiments, isolated brush borders were extracted for 45 min at 4°C with solution A (75 mM KCl, 5 mM $MgCl_2$, 1 mM EGTA, 10 mM imidazole-HCl, pH 7.2; Keller and Mooseker, 1982) containing the protease inhibitors in the presence or absence of 1% (vol/vol) Triton X-100 or 0.6 M KI before preparing a supernate and pellet fraction by centrifugation at 100,000 *g* for 60 min. Samples for PAGE and Western blotting were prepared from these various fractions by adding concentrated SDS gel sample buffer containing dithiothreitol and boiling for 3 min. Espin was detected by Western blotting using affinity-purified rabbit polyclonal antibodies directed against the COOH-terminal 379–amino acid peptide of the ~110-kD rat Sertoli cell espin isoform followed by ^{125}I–protein A (Bartles et al., 1996). The amount of espin present in isolated small intestinal brush borders was determined by scanning laser densitometric analysis of Western blot autoradiograms and comparison to a standard curve generated from internal standards containing known amounts of recombinant small espin (see below). The amount of actin present in the isolated small intestinal brush borders was determined by scanning laser densitometric analysis of Coomassie blue–stained SDS gels and comparison to a standard curve generated from internal standards containing known amounts of rabbit skeletal muscle actin (Cytoskeleton, Inc., Denver, CO).

A cDNA (1,088-bp) that included the full coding sequence of the small isoform of espin was obtained using the affinity-purified rabbit polyclonal antibodies to screen a 5′-STRETCH rat kidney λgt11 cDNA library (CLONTECH Laboratories, Palo Alto, CA). cDNAs were introduced into the pBluescript SK phagemid vector (Stratagene, La Jolla, CA), and the coding and noncoding strands were sequenced in their entirety using [^{35}S]dATPαS and the Sequenase Version 2.0 kit (Amersham Corp., Arlington Heights, IL). Sequence analysis and database searching were carried out using the programs available through the University of Wisconsin Genetics Computer Group (GCG) Sequence Analysis Software Package (Devereux et al., 1984) and the BLAST Search (Altschul et al., 1990) available through the National Center for Biotechnology Information. Peptides with a high probability to form a coiled coil were identified using the programs of Lupas (1997) and Berger et al. (1995).

For immunoperoxidase labeling, rat intestine and kidney were fixed by perfusion through the abdominal aorta with Bouin's fluid and embedded in paraffin (Bartles et al., 1996). 5-μm sections were deparaffinized with xylenes, labeled with affinity-purified rabbit polyclonal espin antibody or preimmune IgG followed by horseradish peroxidase–conjugated donkey anti–rabbit $F(ab')_2$, reacted with H_2O_2 and 3,3′-diaminobenzidine, and counterstained with hematoxylin (Bartles et al., 1996). In preparation for immunofluorescence, isolated small intestinal brush borders were fixed to poly-L-lysine–coated slides or coverslips with 2% paraformaldehyde in solution A containing 20 mM Hepes, pH 7.2, and 20 mM *n*-octyl-β-D-glucopyranoside, quenched with 0.25% (wt/vol) NH_4Cl and 0.5% (wt/vol) BSA and labeled with affinity-purified polyclonal espin antibody or preimmune IgG and fluorescein-labeled phalloidin (Molecular Probes, Eugene, OR) followed by rhodamine-labeled goat anti–rabbit IgG (Jackson ImmunoResearch Laboratories, Inc., West Grove, PA) in PBS containing 0.02% (wt/vol) saponin (Bartles et al., 1996). In preparation for postembedment immunogold labeling, freshly isolated rat small intestinal brush borders were washed twice by low-speed centrifugation in 60 mM Pipes, 25 mM Hepes, 10 mM EGTA, 2 mM $MgCl_2$, pH 6.9, containing the protease inhibitors, fixed for 30 min at 4°C in the same buffer containing 4% paraformaldehyde, pelleted by centrifugation at 13,000 *g* for 20 min, post-fixed as a pellet for an additional 1.5 h at 4°C, washed overnight with two

Published October 5, 1998

changes of the same buffer minus paraformaldehyde, dehydrated through 30, 50, and 70% ethanol at −20°C, infiltrated overnight with LR white (Electron Microscopy Sciences, Ft. Washington, PA) at 4°C with eight changes, placed in gelatin capsules, and then polymerized for 3–5 d at 38–40°C. Ultrathin sections were quenched with 0.5% (wt/vol) BSA in Tris-buffered saline, pH 7.4, and labeled for 15 h with affinity-purified espin antibody or preimmune IgG followed by goat anti–rabbit IgG 12- or 6-nm-diameter colloidal gold conjugate (Jackson ImmunoResearch Laboratories) and counterstained with 2–3% (wt/vol) uranyl acetate. To minimize aggregation of the gold conjugate, the tracer was blended thoroughly on a vortex mixer and then precleared by centrifugation at 13,000 *g* for 5 min immediately before use. For preembedment immunogold labeling, isolated rat small intestinal brush borders were fixed in 4% paraformaldehyde in solution A containing 20 mM Hepes, pH 7.2, and 0.5% (vol/vol) Triton X-100, quenched with 0.25% (wt/vol) NH_4Cl and 0.5% (wt/vol) BSA, and labeled in suspension with affinity-purified espin antibody or preimmune IgG followed by colloidal gold–labeled secondary antibody (see above). In between steps, the brush borders were washed by low-speed centrifugation. After the final wash, the labeled brush borders were postfixed in 2% glutaraldehyde in 0.1 M sodium cacodylate, pH 7.4, postfixed in 1% OsO_4, stained en bloc with uranyl acetate, dehydrated in ethanol and propylene oxide, and embedded in Poly/Bed 812 (Polysciences, Warrington, PA). Ultrathin sections were stained with uranyl acetate and lead citrate.

For transient transfection, the 1,088-bp cDNA encoding small espin was introduced into the EcoRI site of the pEGFP-C2 vector (CLONTECH Laboratories) and used to express a green fluorescent protein (GFP)[1]–small espin fusion protein in cells of the BHK fibroblastic line (American Type Culture Collection, Rockville, MD) by transient transfection with lipofectamine (Life Technologies, Gaithersburg, MD). The cells were cultured on coverslips in DME containing 10% (vol/vol) calf serum and penicillin/streptomycin. The GFP–small espin fusion protein was localized in these cells by conventional fluorescence microscopy, either without fixation or after fixation with 2% paraformaldehyde in PBS, pH 7.4, extraction for 5 min with ice-cold 0.1% (vol/vol) Triton X-100 in PBS, and labeling with rhodamine-phalloidin (Molecular Probes). In some transfection experiments, small espin was expressed without GFP, using the pcDNA3 expression vector (Invitrogen, Carlsbad, CA), and detected by immunofluorescence (Bartles et al., 1996).

cDNAs encoding the full-length small espin protein and NH_2- or COOH-terminally truncated versions were prepared from the library cDNA clone by PCR using Deep Vent DNA polymerase (New England Biolabs, Beverly, MA) with limiting amounts of template and enzyme. Primers were designed to introduce a BamHI site at the 5′ end and an EcoRI and/or a HindIII site at the 3′ end. The cDNAs were introduced into the BamHI and EcoRI or HindIII sites of the pProEX HT prokaryotic expression vector (Life Technologies) that gave the proper reading frame. The resulting constructs were checked by automated DNA sequencing (using a BigDye terminator and model 377 sequencer; Applied Biosystems, Inc., Foster City, CA) and used to transform *Escherichia coli* DH5α (Life Technologies). These resulting recombinant proteins included an additional 28 amino acids at their NH_2 termini: MSYY, followed by HHHHHH (the 6xHis tag), DYDIPTT (a spacer region), ENLYFQ (Tobacco Etch Virus protease cleavage site), and GAMGS. The 6xHis-tagged small espin constructs were isolated from 50 mM Tris-HCl, 10 mM 2-mercaptoethanol, pH 8.5, extracts of frozen-thawed, sonicated bacteria by batch affinity chromatography on Ni-NTA resin (Qiagen, Chatsworth, CA) using the 0.1 M KCl, 10% (vol/vol) glycerol, 10 mM 2-mercaptoethanol, 20 mM Tris-HCl, 20 mM imidazole-HCl, pH 8.5, buffer system recommended by Life Technologies. The 0.2-M imidazole eluate was dialyzed against 0.1 M KCl, 10 mM imidazole-HCl, 1 mM NaN_3, pH 7.4; treated at a concentration of 0.02–0.05 mg/ml with 15 U/ml of recombinant 6xHis-tagged Tobacco Etch Virus protease (Life Technologies) for 3 h at 37°C; incubated for 30 min at 4°C with Ni-NTA resin to remove cleaved 6xHis-tag, any uncleaved 6xHis-tagged small espin, and the residual 6xHis-tagged viral protease; adjusted to 2 mM $MgCl_2$; and freed of any insoluble protein by centrifugation at 150,000 *g* for 90 min at 4°C in preparation for use in F-actin binding and bundling assays. After removal of the 6xHis tag with Tobacco Etch Virus protease, the constructs retained only an extra five amino acids, GAMGS, at their NH_2 terminus.

F-actin was prepared by dilution of purified rabbit skeletal muscle actin or human platelet nonmuscle actin (85% β-actin and 15% γ-actin) (Cytoskeleton, Inc.) into 0.1 M KCl, 2 mM $MgCl_2$, 1 mM ATP, 1 mM NaN_3, 10 mM imidazole-HCl, pH 7.4, and incubation for 60 min at 37°C. To assay for F-actin binding or bundling, an equal volume of solution containing different amounts of recombinant small espin protein in the same buffer minus ATP was added to preformed actin filaments (at a final actin concentration of 0.1–0.5 mg/ml) and incubated for 60 min at 37°C. Samples were either taken for negative staining with 0.5–1% (wt/vol) uranyl acetate on 300-mesh Formvar and carbon-coated copper grids (Cooper and Pollard, 1982) or were centrifuged at 4°C for either 15 min at 22,000 *g* (bundling assay; Edwards et al., 1995) or for 90 min at 150,000 *g* (binding assay; Bartles et al., 1996). The levels of small espin protein and actin present in the supernate and pellet fractions were determined by scanning laser densitometric analysis of Coomassie blue–stained SDS gels using the rabbit skeletal muscle actin as the protein standard.

For sedimentation equilibrium, the purified recombinant espin was dialyzed against 0.1 M KCl, 0.02 M Tris-HCl, 2 mM $MgCl_2$, 1 mM NaN_3, pH 7.4, and centrifuged for 22–24 h at 15,000 rpm in an analytical ultracentrifuge (model XLA-1; Beckman Instruments, Fullerton, CA). The molecular mass was estimated from plots of log A_{280} versus radius squared. The modeling of molecular dimensions (semimajor [a] and semiminor [b] axes multiplied by 2) and sedimentation coefficient using subunit molecular mass and frictional coefficient ratio for three basic asymmetrical shapes (prolate ellipsoid, oblate ellipsoid, and long rod) were carried out using the XL-A-UltraScan-Origin Software Package Version 2.93 produced by Dr. Borries Demeler (Missoula, MT) and supplied with the instrument. To measure sedimentation coefficient, the purified espin was centrifuged for 3 d at 25,000 rpm under isokinetic conditions in a linear 3–15% (wt/vol) sucrose gradient in 0.1 M KCl, 2 mM $MgCl_2$, 10 mM imidazole-HCl, 1 mM NaN_3, pH 7.4. To measure Stokes' radius, the purified espin was chromatographed on a 93 × 1.5-cm column of Sephadex G-100 in the same buffer minus sucrose. The sedimentation coefficient and Stokes' radius were determined by SDS gel analysis of the gradient and column fractions, respectively, with comparison to the protein standards in the MW-GF-1000 gel filtration standards kit plus horse heart cytochrome c (Sigma Chemical Co., St. Louis, MO). The small espin was examined in SDS gels before and after centrifugation or gel filtration to ensure that it had not undergone proteolysis during the procedure. Circular dichroism spectroscopy was carried out at room temperature at rate of 50 nm/min using a freshly calibrated spectropolarimeter (model J-715; Jasco, Inc., Easton, MD) on samples containing ~50 μg/ml of purified small espin in 50 mM NaP_i, pH 7.4, in a 0.1-cm path length cell. Molecular cross-linkers were purchased from Pierce Chemical Co. (Rockford, IL).

Results

Identification and Sequence Analysis

To determine whether the ~1.7-kb crosshybridizing RNAs detected previously in our Northern blot analysis of total RNA isolated from rat kidney and small intestine (Bartles et al., 1996) encoded espin-related proteins, homogenates of rat kidney and small intestinal mucosa were compared with homogenate of rat testis on Western blots using affinity-purified rabbit polyclonal antibody directed against the COOH-terminal 379–amino acid peptide of rat Sertoli cell espin. In addition to reacting with the ~110-kD Sertoli cell espin band present in homogenate of testis, the espin antibody also specifically labeled a closely spaced doublet of ~30-kD present in homogenate of rat kidney and small intestinal mucosa (Fig. 1 *A*).

To elucidate the sequence of the ~30-kD protein detected by Western blotting, the espin antibody was used to screen a commercial rat kidney cDNA library. A single 1,088-bp cDNA clone was obtained, and its sequence was determined. The single large open-reading frame present in this cDNA began at nucleotide 63, in the context of a Kozak consensus sequence (Kozak, 1987), and was predicted to encode a small version of the espin protein that was ~1/3 the size of Sertoli cell espin, 253 amino acids ver-

1. *Abbreviation used in this paper*: GFP, green fluorescent protein.

Published October 5, 1998

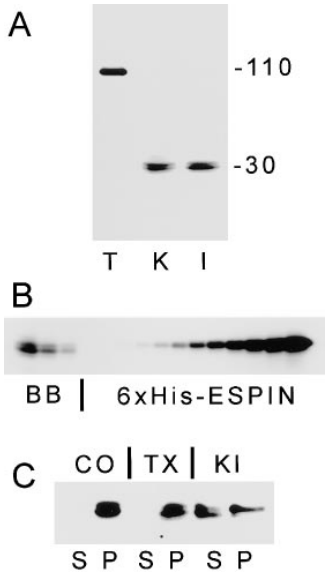

Figure 1. Detection, quantification, and extraction of small espin. (*A*) Western blot of homogenate of rat testis (*T*), kidney (*K*), and small intestinal mucosa (*I*) using espin antibody (apparent molecular mass depicted on right in units of kD). (*B*) Western blot quantification of small espin in isolated rat small intestinal brush borders, comparing brush border (*BB*) samples containing (from left to right) 40, 20, and 10 μg of actin and (from right to left) serial twofold dilutions of recombinant small espin (*6xHis-ESPIN*) internal standard starting with 3.2 μg in the far right lane. (*C*) Western blot of high-speed supernate (*S*) and pellet (*P*) resulting from the extraction of isolated rat small intestinal brush borders in solution A in the absence (*CO*) or presence of 1% (vol/vol) Triton X-100 (*TX*) or 0.6 M KI for 45 min at 4°C.

sus 837 amino acids,[2] with a molecular mass of 28,240 D and an isoelectric point of 10.5. Attempts at 5′ rapid amplification of cDNA ends failed to identify any additional in-frame translation start sites upstream (data not shown), and the recombinant protein encoded by nucleotides 63–821 of this cDNA was found to exhibit the expected apparent molecular mass (~30 kD) in SDS gels (see below). The nucleotide sequence, the predicted amino acid sequence, and a comparison between the small and large espin isoforms are shown in Fig. 2. Along much of its length, small espin was identical in sequence to the COOH-terminal portion of the larger Sertoli cell isoform. As a result, it contained the potential P-loop (A32-S39), the 66–amino acid peptide that showed 39% identity to a peptide encoded by exon A5 and is present in both the large and small forked proteins of *Drosophila* (I140-K205), and the two peptides that contained clusters of multiple glutamates bracketed by arginines, lysines, and glutamines in a pattern reminiscent of the repetitive motif found in the protein trichohyalin (R160-R182 and R195-R219). Small espin did not, however, contain the ankyrin-like repeats and proline-rich peptides present in the large isoform. In their place, it contained a considerably shorter NH_2 terminus with two unique small peptides (M1-P13 and S61-R86) interrupted by another peptide (S14-A60) that was present in the large isoform. When analyzed using the secondary structure algorithms of Chou and Fasman (1978) or those of Garnier et al. (1978), a large fraction of the COOH-terminal half of small espin (R160-A238) was predicted to adopt an α-helical secondary structure. In addition, when analyzed using the algorithms or Lupas (1997) or Berger et al. (1995), two COOH-terminal peptides (Q156-L186 and R190-G231 or L194-G231) were predicted to form a coiled coil with high probability.

A

```
1                                                                  aa 2
3 ttccgggtcgatggtgggcagacatctgctggagtccccagggctggcccgagagccacc 62
63 atgaactcccaggggcctctacgtgggggccgaatgcccagcaccaaatctttcaacatg 122
1 [M N S Q G P L R G G R M P] S T K S F N M 20

123 atgtccccaacgggtgacaactcggagttgctggctgaaataaaagcaggcaagagtctg 182
21 M S P T G D N S E L L A E I K A G K S L 40

183 aaaccaacaccgcagagcaaggggctgacaacagtgttctcaggcagcgggcagccagcc 242
41 K P T P Q S K G L T T V F S G S G Q P A 60

243 tcccaggtaggcactggacgggtgccccgcccgggctcccagtgcctgcccagtgctcag 302
61 [S Q V G T G R V P R P G S Q C L P S A Q 80

303 ccctaccgcttctcccggcagcctgagtcaccacagcctgcggtgtcacctgggccatct 362
81 P Y R F S R] Q P E S P Q P A V S P G P S 100

363 cgggcccggagccccaccccaccagcctctgggcctcagccactgctcaatggcagcata 422
101 R A R S P T P P A S G P Q P L L N G S I 120

423 gtaccggcaccacctgccaccctagcaccaggagtgcatctggatgtggaggccctcatc 482
121 V P A P P A T L A P G V H L D V E A L I* 140

483 cccacacttgatgagcagggccggcccatcccggagtggaagcgccaggtgatggtccgg 542
141 P* T L D* E Q G* R P I* P* E W* K* R* Q* V M* V R 160

543 aagctgcagcagaaaatgcaggaggaagaggagcagcggaggaaggaagaagaggaggag 602
161 K* L Q Q K M Q E E E E* Q R* R K E E* E E* E 180

603 gcccggctggccagcctgcccgcctggagacgagacattcttaggaagaagctggaggag 662
181 A R* L* A S L P* A W* R R* D* I L* R K K L E* E 200

663 gagagggagcagaagcgaaaagaggaggagcggcagaagctggaggaaatccagagggcg 722
201 E* R E Q K* R K E E E R Q K L E E I Q R A 220

723 aaagaacagtcggagaagctgcggacactaggatacgacgaggccaagctcgcgccctgg 782
221 K E Q S E K L R T L G Y D E A K L A P W 240

783 cagcgacaggtcatcttgaagaaggggagatccctaagtaataggagtctcggcctctt 842
241 Q R Q V I L K K G E I P K 253

843 gcgtgtagcctcacgagctctgagaaatggggagcggccccagcccccgccccatcctg 902
903 tcaggttggtgcggaagggtgggagccttgagcccttcccttcggtgcctgccggaatct 962
963 tccctattcccctccctggccccacatccccaaccctgctgctggagtgctctcgcgaac 1022
1023 ccctgctgtcgcctggaaaaaaaaagtgcccaggctgctgacgcaaaaaaaaaaaaagg 1082
1083 ccttaa 1088
```

B

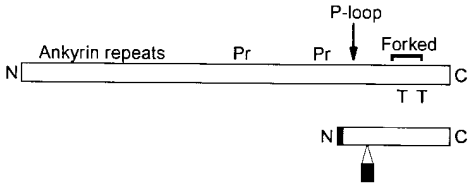

Figure 2. Sequence of small espin and its relationship to the large isoform. (*A*) The cDNA and amino acid sequence of rat small espin. The peptides unique to the small isoform (M1-P13 and S61-R86) are enclosed in brackets. The amino acids in the forked homology peptide (I140-K205) that are identical to those in the forked protein are marked with an asterisk. (*B*) Diagram depicting (approximately to scale) the structural relationships between the large and small isoforms of espin and some of their known motifs (*Pr*, proline-rich peptides; *T*, peptides with trichohyalin-like repeats). The peptides unique to the small isoform are shaded. These sequence data are available from GenBank/EMBL/DDBJ under accession number AF076856.

2. We have discovered three errors in the sequence of the large isoform between nucleotides 1835 and 1907 (Bartles et al., 1996). These errors have been corrected in the database (available from GenBank/EMBL/DDBJ under accession number U46007). The corrections bring about a shift in reading frame over a span of 22 amino acids and result in the addition of one amino acid. The corrected total number of amino acids for the large isoform is 837, and the corrected amino acid sequence for this region is: 607-GAGAACGQRRSSSSTGSTKSFNMMSPTG-634.

Published October 5, 1998

Localization, Quantification, and Solubility

When localized at the light-microscopic level using the immunoperoxidase technique, small espin was found to be concentrated over the F-actin–rich brush borders of absorptive epithelial cells in the small intestine and kidney (*arrowheads* in Fig. 3, *A* and *B*, respectively). On sections of rat small intestine, some weaker labeling was also detected more basally within enterocytes. Compared with the brush borders of the mature enterocytes on intestinal villi, the apical margins of the enterocyte precursors found within the crypts of Lieberkühn (e.g., Fig. 3 *A*, *arrow*) had considerably lower levels of labeling. This suggested that small espin was expressed or accumulated in a developmental fashion during the assembly of the brush border (Ezzell et al., 1989; Heintzelman and Mooseker, 1992; Fath and Burgess, 1995). On sections of rat kidney, only the epithelial cells lining the distal straight portion of the proximal tubule near the cortico-medullary junction, presumably corresponding to segment S3 (Kriz and Kaissling, 1992), showed intense labeling along their brush borders (Fig. 3 *B*). Proximal convoluted tubules near glomeruli in the renal cortex showed considerably less labeling (data not shown). The proximal tubular epithelial cells with intensely labeled brush borders appeared to have an even higher level of cytoplasmic labeling than the enterocytes.

The majority (83–86%) of small espin present in homogenates of rat kidney and small intestinal mucosa resisted extraction with 1% (vol/vol) Triton X-100 (data not shown). Small espin was recovered in isolated rat small intestinal brush borders, where it was colocalized with F-actin at the light-microscopic level (Fig. 4, *A–C*). On the basis of quantitative Western blotting, we could estimate that ~1 small espin was recovered for every 130 actin monomers in small intestinal brush borders isolated from adult rats. Fig. 1 *B* shows a Western blot in which dilutions of isolated rat small intestinal brush borders containing known amounts of actin are compared with internal standards containing known amounts of recombinant small espin (see below). Consistent with an association between small espin and the actin cytoskeleton, the small espin present in the isolated rat small intestinal brush borders resisted extraction with 1% (vol/vol) Triton X-100 but could be partially extracted with 0.6 M KI (Fig. 1 *C*).

Post- and preembedment immunogold electron microscopy were used to examine the localization of the small espin recovered on the isolated rat small intestinal brush borders at a higher level of resolution. When LR white sections of paraformaldehyde-fixed brush borders were labeled with affinity-purified polyclonal espin antibody followed by secondary antibody–colloidal gold conjugate, the bound gold particles were observed over the microvilli proper and over the actin bundles of the microvillar rootlets, but not over the terminal web (Fig. 4 *D*). Neither the sections labeled with preimmune IgG instead of the espin antibody nor the occasional nuclear fragment that can contaminate this subcellular fraction showed bound gold

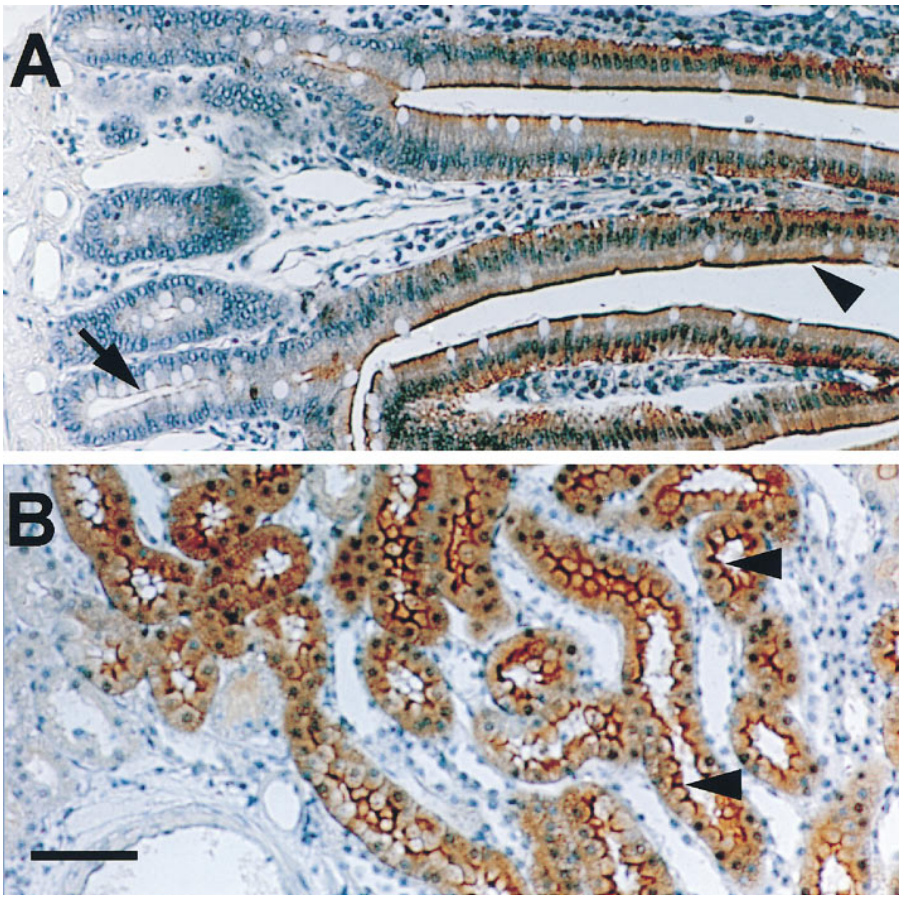

Figure 3. Immunoperoxidase localization of small espin in rat small intestine (*A*) and kidney (*B*). Arrowheads denote the positions of intense brush border staining. The arrow in *A* shows an example of reduced immunolabeling on enterocyte precursors in a crypt of Lieberkühn. Bar, 100 μm.

Published October 5, 1998

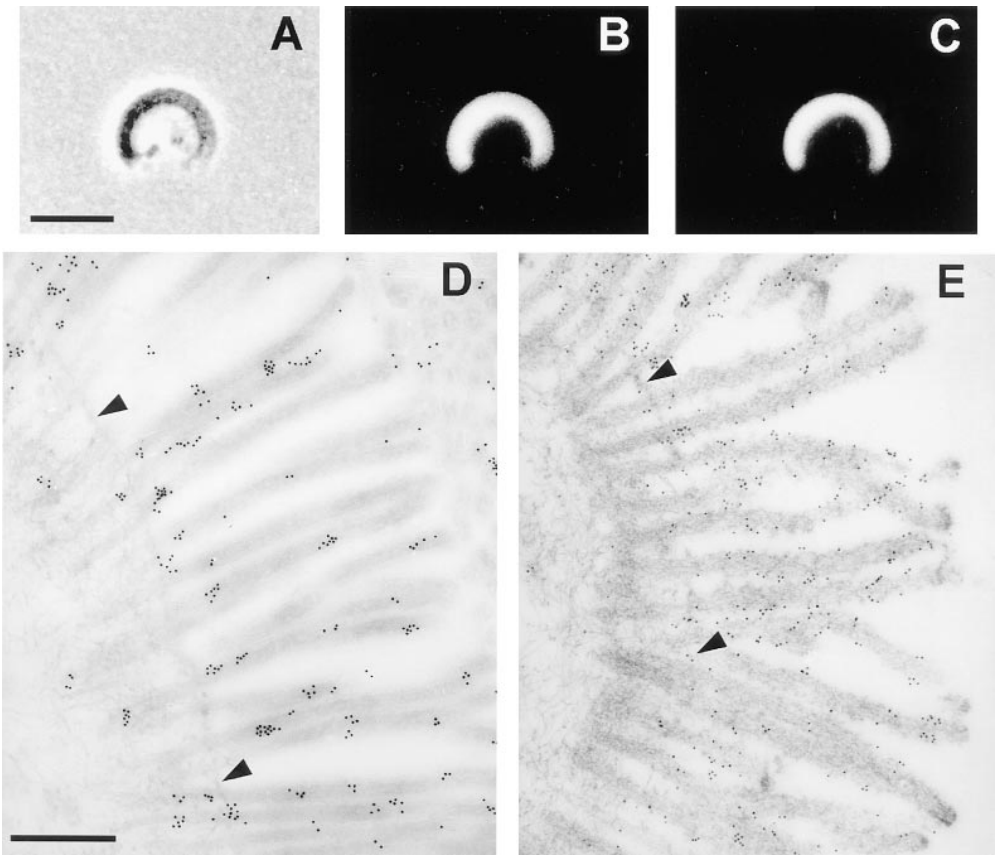

Figure 4. Localization of small espin on isolated rat small intestinal brush borders. (*A–C*) Immunofluorescence localization of espin (*B*) compared with that of F-actin, as revealed using fluorescent phalloidin (*C*), and to the phase contrast image (*A*). Postembedment (*D*) and preembedment (*E*) immunogold localization. The rootlets lie to the left of the arc traced out by the intermicrovillar plasma membrane (*arrowheads*). Bars: (*A*) 5 μm; (*D*) 0.4 μm.

particles (data not shown). After examining more than 250 brush border profiles, we concluded that the specifically bound gold particles could be found anywhere along the length of the microvillar actin bundle. Preembedment immunogold labeling (Fig. 4 *E*) indicated that a significant pool of small espin was accessible to primary antibody and secondary antibody–colloidal gold conjugate in isolated brush borders that were fixed with paraformaldehyde in the presence of Triton X-100. Specimens labeled with preimmune IgG instead of espin antibody showed no bound gold particles (not shown). Compared with postembedment labeling, the specifically bound gold particles appeared to be more evenly distributed along microvilli, but fewer gold particles were detected over rootlets, suggesting that there was reduced accessibility of the tracer using the preembedment technique. Comparable results were obtained when the diameter of the secondary antibody–colloidal gold was reduced from 12 to 6 nm (data not shown).

Transfection

To obtain additional evidence in support of an interaction between small espin and the actin cytoskeleton in vivo, we examined the localization of a GFP–small espin fusion protein in transiently transfected cells of the BHK fibroblastic line. On the basis of immunofluorescence and Western blotting (not shown), these cells were judged not to contain significant amounts of espin in the absence of transfection. When living cells were examined by conventional fluorescence microscopy 1 d after transfection, the GFP–small espin fusion protein was observed to decorate fine (Fig. 5 *A*) or more coarse (Fig. 5, *B* and *C*) stress fiber–like structures, whereas GFP without the small espin attached was found to be distributed more diffusely throughout the cytoplasm with evidence of concentration within the nucleus (Fig. 5 *B*, *inset*). To further examine the identity of the GFP–small espin–labeled fibers observed in living cells, the cells were fixed with paraformaldehyde, permeabilized with Triton X-100 and double labeled with rhodamine-phalloidin as a marker for F-actin. The patterns of GFP–small espin (Fig. 5 *D*) and rhodamine-phalloidin (Fig. 5 *E*) were found to be coincident, suggesting that exogenous small espin was associating with F-actin–containing structures in the transfected cells. In contrast, GFP without the small espin attached was detected in perinuclear aggregates in the fixed and permeabilized cells (Fig. 5 *D*, *inset*). Interestingly, the level of F-actin, as reflected by the intensity of rhodamine-phalloidin labeling, was consistently higher in cells expressing GFP–small espin than in the corresponding untransfected control cells (Fig. 5 *E*) or in cells expressing GFP alone (not shown). This latter result suggested that small espin could elicit the accumulation and/or bundling of F-actin–containing fibers or cables in the transfected cells. Neither the apparent accumulation of these F-actin–containing structures nor their decoration with small espin required the presence of the GFP because the same results were obtained when

Published October 5, 1998

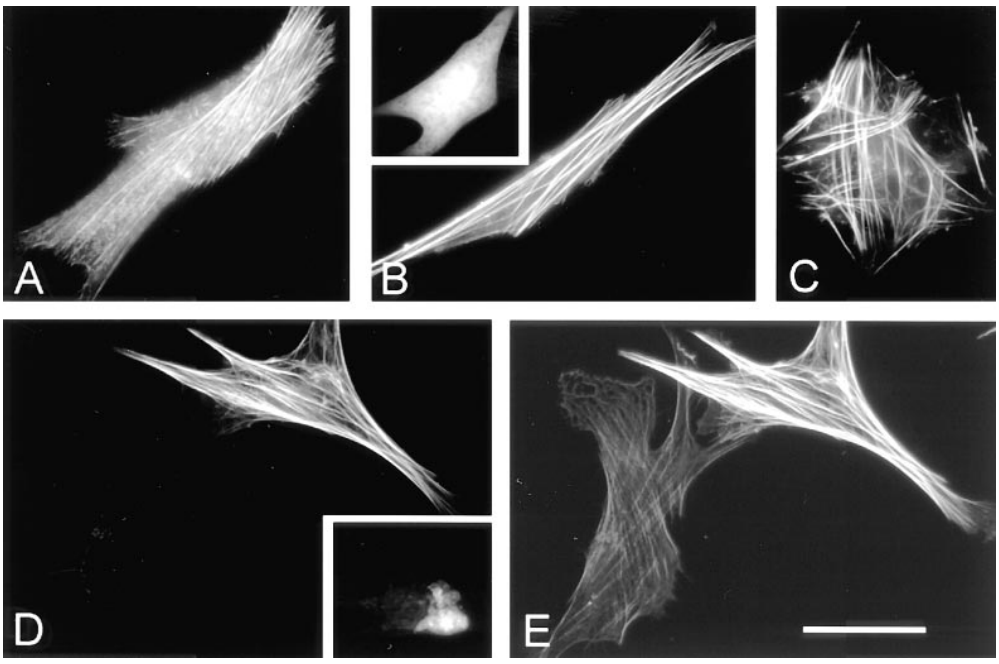

Figure 5. Localization of GFP–small espin in transiently transfected BHK cells. (*A–C*) GFP espin in living cells. (*B*, *inset*) Control with GFP alone. (*D* and *E*) Fixed and permeabilized cells examined for GFP–small espin (*D*) or F-actin, as revealed by rhodamine-phalloidin (*E*). (*D*, *inset*) Control with GFP alone. Bar, 25 μm.

small espin was expressed without the GFP using the pcDNA3 vector and was detected by immunofluorescence (data not shown).

Bacterial Expression and Actin Binding/Bundling In Vitro

To examine the properties of small espin and its interactions with F-actin under defined conditions in vitro, it was necessary to obtain relatively large amounts of the purified protein. Since small espin was difficult to extract from organ/tissue homogenates and isolated brush borders (see above), we elected to use recombinant small espin for these studies. A full-length version of small espin containing a 28–amino acid NH_2-terminal extension that included a 6xHis tag was expressed in *E. coli* and purified by affinity chromatography on Ni-NTA agarose under nondenaturing conditions. The 6xHis tag was released from the protein by cleavage with recombinant 6xHis-tagged Tobacco Etch Virus protease, and the protein, which now contained only five extra amino acids (GAMGS) at its NH_2 terminus, was quickly repurified by a second challenge with Ni-NTA agarose before use.

The purified recombinant full-length small espin was found to bind to and bundle F-actin at physiological ionic strength and pH. This is illustrated in the left part of Fig. 6 *A*, where the supernate and pellet fractions resulting from an F-actin–bundling assay, which uses low-speed centrifugation to separate bundles from preformed actin filaments, were analyzed in an SDS gel. In the absence of small espin, the vast majority of the rabbit skeletal muscle F-actin remained in the supernate fraction upon low-speed centrifugation. However, when the small espin was added to the F-actin (in this case, at a molar ratio of approximately one espin/seven actin monomers), the solution became noticeably turbid, and the vast majority of the

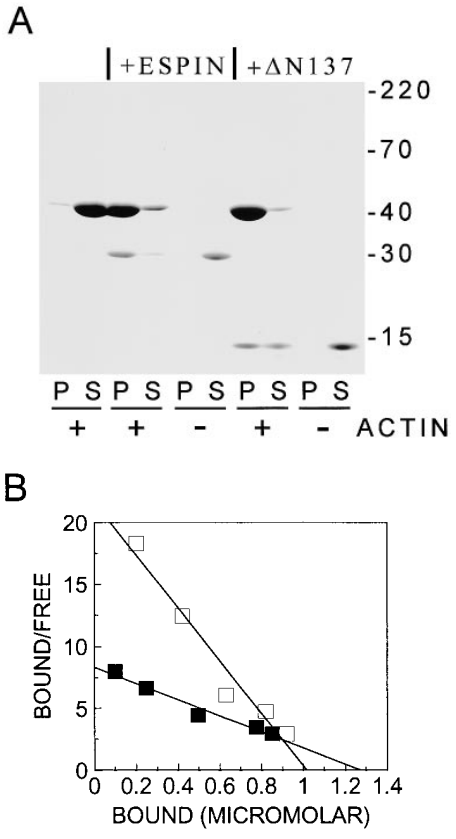

Figure 6. Actin binding and bundling by recombinant small espin. (*A*) Coomassie blue–stained SDS gel of the pellet (*P*) and supernate (*S*) that result from low-speed centrifugation when rabbit skeletal muscle F-actin is incubated alone or in the presence of recombinant small espin (*ESPIN*) or the NH_2-terminal deletion construct ΔN137 for 1 h at 37°C (apparent molecular mass is depicted at the right in units of kD). (*B*) Scatchard plot analysis for the binding of recombinant small espin to rabbit skeletal muscle (*filled*) or human nonmuscle (*open*) F-actin.

Published October 5, 1998

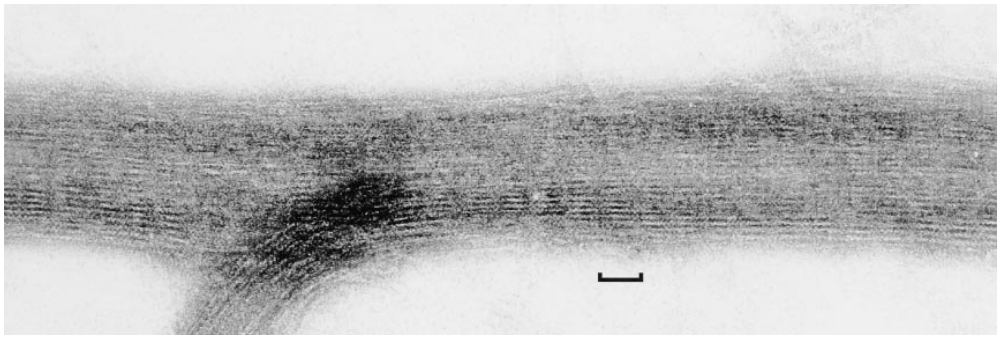

Figure 7. Negative staining electron microscopy of bundle formed by small espin and rabbit skeletal muscle F-actin when mixed at a molar ratio of approximately one espin per seven actin monomers for ~1 h at 37°C. Bar, 36 μm.

F-actin and the small espin were obtained as higher molecular weight cross-linked structures (bundles) in the pellet. In contrast, in the absence of F-actin, the small espin remained in the supernate. When examined by negative staining electron microscopy, the vast majority of the actin filaments present in the small espin/F-actin mixtures were found to be assembled into bundles (Fig. 7). In contrast, the F-actin controls contained randomly oriented actin filaments but no discernible bundles (data not shown). The small espin–induced bundles were partially ordered, frequently showing extended segments with transverse striations, aligned imperfectly across the width of the bundle, at integral multiples of ~12 nm, which is characteristic of maximally cross-linked, hexagonally packed filaments (e.g., see Stokes and DeRosier, 1991; Tilney et al., 1995). Unlike the situation for many other actin-bundling proteins, which display actin-bundling activities that are inhibited by Ca^{2+}(Glenney et al., 1981; Alicea and Mooseker, 1988; Namba et al., 1992; Lin et al., 1994), concentrations of $CaCl_2$ up to 1 mM had no effect on the bundling of F-actin by small espin in the low-speed centrifugation assay (data not shown). And, unlike the bundling of F-actin that results from counterion condensation by positively charged ions and small peptides (Tang and Janmey, 1996), relatively high concentrations of negatively charged small molecules, e.g., 10 mM ATP, also had no effect on the bundling caused by small espin (not shown).

To determine the affinity of the interaction between recombinant small espin and F-actin, high-speed centrifugation was substituted for the low-speed centrifugation to cause all of the F-actin to be recovered in the pellet. The data resulting from the comparison of high-speed pellet and supernate fractions at different inputs of small espin were used to construct Scatchard plots. As is illustrated in Fig. 6 *B*, the recombinant small espin was found to bind to human platelet nonmuscle F-actin with a threefold higher affinity than to rabbit skeletal muscle F-actin. The K_d for nonmuscle F-actin was determined to 50 nM, whereas the K_d for skeletal muscle F-actin was 150 nM. From the intercepts of the resulting linear regression lines on the abscissa, it could be calculated that the binding reached saturation at approximately one espin for every three to four actin monomers.

Oligomeric State, Shape, and Secondary Structure

To further elucidate the mechanism of actin bundling by small espin, we used sedimentation equilibrium to determine whether the purified recombinant small espin was a monomer, dimer or higher oligomer. From the slope of plots of log A_{280} versus radius squared at equilibrium (e.g., Fig. 8 *A*), the molecular mass was estimated to be 25,500 D, only ~12% below the value of ~29,000 D (28,240 D + NH_2-terminal GAMGS) calculated on the basis of sequence, suggesting that recombinant small espin was a monomer. In further support of a monomeric structure for recombinant small espin, we failed to observe covalently cross-linked dimers or higher oligomers when the purified protein was reacted with molecular cross-linkers, such as 3,3′-dithiobis(sulfo-succinimidyl propionate) and 1,5-difluoro-2,4-dinitrobenzene, and analyzed in SDS gels (data not shown).

Given that recombinant small espin appeared to be a monomer, it was found to have an unexpectedly large Stokes' radius by gel filtration. When chromatographed in columns of Sephadex G-100, the recombinant small espin eluted only one fraction after bovine serum albumin, a standard protein with more than twice the subunit molecular mass (66 kD), and seven fractions before carbonic anhydrase, a standard protein with approximately the same subunit molecular mass (29 kD) (Fig. 8 *B*). From the plot of logarithm of the Stokes' radius versus peak elution fraction for the standard proteins (Fig. 8 *B*, *inset*), the Stokes' radius of recombinant small espin was estimated to be 3.4 nm, suggesting that it had a frictional coefficient ratio (f/f_o) of 1.7 and was, therefore, an asymmetrical molecule. For example, it is possible to calculate that a frictional coefficient ratio of 1.7 for a protein of ~29,000 D (28,240 D + NH_2-terminal GAMGS) is compatible with an oblate ellipsoid with dimensions of 10 × 0.6 nm, a prolate ellipsoid with dimensions of 23 × 1.8 nm, or a long rod with dimensions of 17 × 1.2 nm. Using the molecular mass of the small espin monomer and the frictional coefficient ratio of 1.7, one can estimate that the protein should have a sedimentation coefficient of ~2 S. The sedimentation coefficient of the recombinant small espin was measured directly by centrifugation under isokinetic conditions in sucrose density gradients (Fig. 8 *C*). From a plot of sedimentation coefficient versus peak fraction for the standard proteins (Fig. 8 *C*, *inset*), the sedimentation coefficient of small espin was determined to be 2.1 S, just slightly above the predicted value. The observation that small espin sedimented significantly slower than the 29-kD protein carbonic anhydrase, the standard protein with approximately the same molecular mass, also supported the conclusion that small espin was an asymmetrical monomer.

When examined by far-UV circular dichroism spectros-

Published October 5, 1998

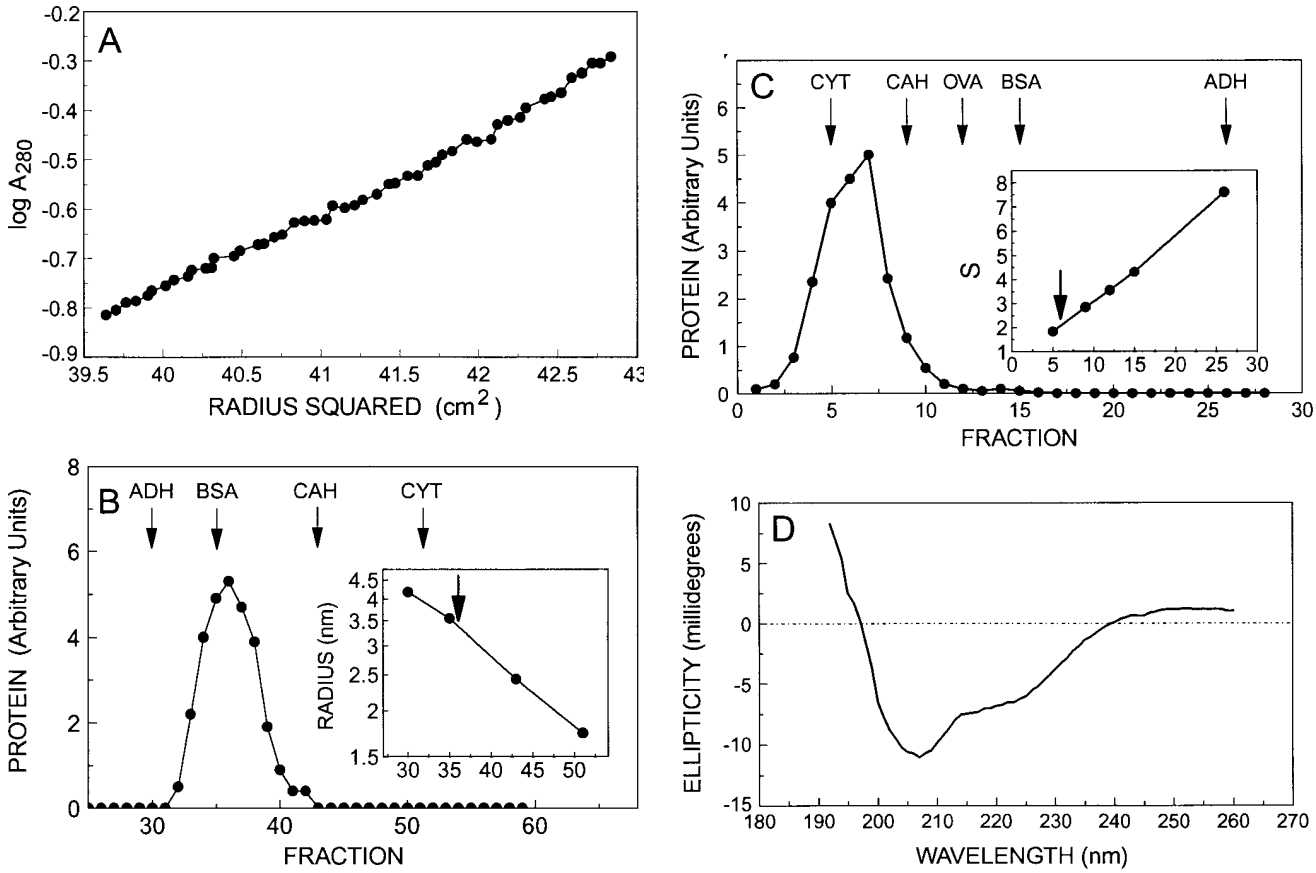

Figure 8. Physical properties of recombinant small espin. (*A*) Sedimentation equilibrium: plot of log A_{280} versus radius squared at equilibrium (slope = 0.16, correlation coefficient = 0.993). (*B*) Gel filtration in Sephadex G-100 relative to standards (*ADH*, yeast alcohol dehydrogenase; *BSA*, bovine serum albumin; *CAH*, bovine carbonic anhydrase; *CYT*, horse cytochrome c). (*Inset*) Semilog plot of Stokes' radius versus peak elution fraction. (*C*) Sedimentation in sucrose density gradient relative to standards (*OVA*, ovalbumin standard). (*Inset*) Plot of sedimentation coefficient (*S*) versus peak fraction. (*D*) Circular dichroism spectrum.

copy, the spectrum of the purified full-length recombinant small espin had large negative peaks at 220 and 207 nm and a large positive peak at 192 nm (Fig. 8 *D*), corresponding to the major n-π* and π-π* transitions displayed by α-helices (Chen et al., 1974). These results suggested that the recombinant small espin was a highly folded protein and that, as predicted on the basis of sequence (see above), it contained a high percentage of α-helix. Unlike the spectra of many other α-helical proteins, however, the negative peak at 207 nm was significantly larger than the one at 220 nm, suggesting that the helical region was relatively long (>50 amino acids; Chen et al., 1974) and/or that, despite the prediction of a coiled-coil structure (see above), its various helical segments did not interact with one another (e.g., Zhou et al., 1992; Su et al., 1994).

Deletion Mapping of the Actin-bundling Peptide

PCR was used to generate a series of small espin NH_2- or COOH-terminal deletion constructs with NH_2-terminal 6xHis tags to allow for ready purification. The sequences of these constructs were verified by automated DNA sequencing, and the constructs were compared in the low-speed centrifugation actin-bundling assay after removal of the 6xHis tag and repurification. Deletion of the NH_2 terminus up to the 167–amino acid COOH-terminal peptide shared by the Sertoli cell and brush border isoforms (ΔN86), or up to the beginning of the forked homology domain (ΔN137), produced recombinant proteins that displayed actin-bundling activities equal to, or perhaps slightly greater than, that of full-length small espin (Fig. 9). An example of an SDS gel depicting the results of an actin-bundling assay for construct ΔN137 is shown on the right side of Fig. 6 *A*. Further deletion from the NH_2 terminus, up to the middle of the forked homology peptide (ΔN170), caused a dramatic (80-fold) decrease in actin-bundling activity to near background levels (Fig. 9). Deleting the last 5 amino acids from the COOH terminus of small espin (ΔC5) had no effect on actin-bundling activity, but deletion of an additional 13 amino acids (ΔC18), or deletion of a total of 73 amino acids from the COOH terminus (ΔC73), also caused a dramatic decrease in actin-bundling activity to near background levels (Fig. 9). These results suggested that the COOH-terminal 116–amino acid peptide common to the two known isoforms of espin (A138-K253 in small espin) was sufficient to cause maximum actin bundling in vitro. Since small espin was found to be a monomer in solution (see above), the COOH-ter-

Published October 5, 1998

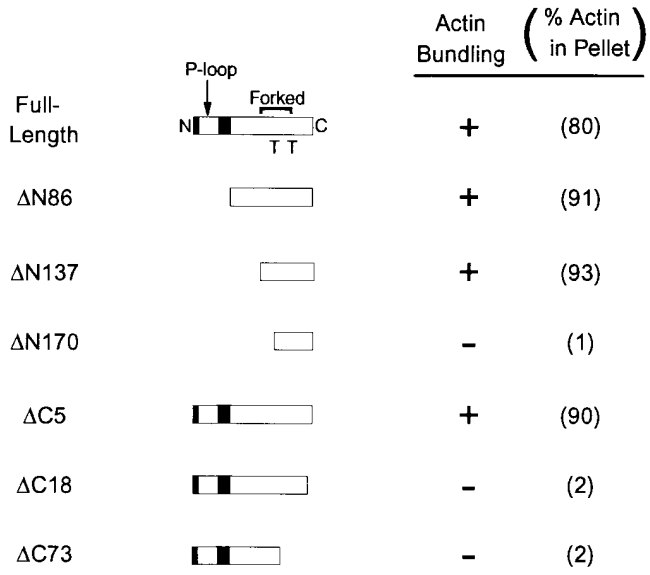

Figure 9. Actin bundling activity of NH_2- or COOH-terminal deletion constructs of small espin. + or − signifies the presence or absence of actin-bundling activity for the designated construct as determined by qualitative analysis of the SDS gels that resulted from the low-speed centrifugation assay (see Fig. 6 *A*). The assays were conducted on at least three independent isolates of each recombinant protein at a molar ratio of approximately one espin per seven actin monomers. The numbers shown in parentheses specify the percent of the actin recovered in the low-speed pellet in a single experiment in which all seven constructs were compared and the SDS gel was analyzed by laser densitometry. These numbers have been corrected for the ~2% of actin that was recovered in the pellet in the absence of espin construct. In the accompanying diagrams, the two NH_2-terminal peptides specific to the small isoform have been shaded.

minal 116–amino acid peptide must presumably contain two or more actin-binding sites. The dramatic losses in actin-bundling activity observed in going from ΔN137 to ΔN170 and from ΔC5 to ΔC18 suggested further that the 33–amino acid peptide at the NH_2 terminus of the forked homology peptide (A138-E170) and the 13–amino acid peptide K236-K248 were necessary for bundling activity and, therefore, may contribute to the formation of small espin's actin-binding sites.

Discussion

Taken together, our data strongly support the hypothesis that small espin is a newly identified actin-bundling protein of the brush border. Small espin is localized to the parallel actin bundles of brush border microvilli, and it accumulates there coincident with the migration/differentiation of enterocytes along the crypt–villus axis in the adult. The protein is recovered in the Triton X-100–insoluble cytoskeletal fraction prepared from isolated brush borders. Recombinant small espin binds to F-actin with high affinity, and it cross-links the actin filaments into partially ordered bundles. The recombinant small espin protein is a monomer in solution and appears to contain at least two relatively closely spaced actin-binding sites. And finally, when expressed exogenously in transfected fibroblastic cells, small espin decorates F-actin fibers and cables and appears to cause their accumulation, suggesting that small espin can bind to, stabilize, and/or bundle F-actin in vivo.

The Espin Family and the Mechanism of Espin-mediated Actin Bundling

Small espin showed no significant sequence similarity to other proteins known or suspected to bind/bundle F-actin, with the exception of the large isoform of espin and the forked proteins of *Drosophila*. With the identification of the small isoform of espin, it is clear that the espins constitute a new family of actin-binding/bundling proteins. The two members of the espin family we have described thus far, the 837–amino acid ectoplasmic specialization isoform (Bartles et al., 1996) and the 253–amino acid brush border isoform, are expressed in different cell types and are markedly different in size. Nevertheless, both isoforms are localized to specializations of the cell surface, an invagination or an evagination, that contain hexagonally packed parallel actin bundles, and both contain an identical COOH-terminal 167–amino acid peptide that is sufficient to bundle F-actin in vitro. The observation that the peptides specific to the small isoform (M1-P13 and S61-R86) are found interspersed among peptides identical in sequence to those present in the large isoform suggest that the two espin isoforms arise through differential splicing. We are currently investigating the organization of the espin gene(s) and comparing the properties and activities of the small and large isoforms to ascertain how their different NH_2 termini influence interactions with F-actin.

Although small espin is a basic protein and contains many highly charged peptide segments, the fact that the bundling took place in 0.1 M KCl at pH 7.4 and was not inhibited by a small, highly charged anion, in this case up to 10 mM ATP, suggests that the bundling is due to the presence of specific actin-binding sites in small espin and is not the result of counterion condensation (Tang and Janmey, 1996). Through deletion mutagenesis, we established that the COOH-terminal 116–amino acid peptide shared by the two espin isoforms was sufficient to cause maximal actin bundling in the low-speed centrifugation assay. Since small espin proved to be a monomer in solution, this suggests that the COOH-terminal 116–amino acid peptide contains two, or possibly more, actin-binding sites. The simplest model that can account for the dramatic losses in actin-bundling activity noted in going from ΔN137 to ΔN170 and from ΔC5 to ΔC18 is one in which small espin contains two actin-binding sites disposed roughly at opposite ends of the COOH-terminal 116–amino acid peptide. Our sedimentation and gel filtration analyses suggest that small espin is a relatively small, asymmetrical molecule with dimensions in the range of 10–23 × 0.6–1.8 nm. Further experiments are underway to elucidate the three-dimensional structure of small espin and to map its actin-binding sites and its footprint on F-actin at high resolution.

Relationship between the Espins and the Forked Proteins of Drosophila

The dramatic loss in the actin-bundling activity of small espin noted in going from ΔN137 to ΔN170 suggests that the NH_2-terminal half of its 66–amino acid forked homology

Published October 5, 1998

peptide is necessary for actin-bundling activity and may therefore be important in forming one of small espin's actin-binding sites. This lends support to the hypothesis (Bartles et al., 1996) that the espins and the forked proteins are orthologous families of proteins. Although, to our knowledge, no forked protein has yet been observed to bundle F-actin directly, genetic studies have demonstrated that the forked proteins are necessary to form normal actin bundles in the developing bristles of *Drosophila* pupae (Hoover et al., 1993; Petersen et al., 1994; Tilney et al., 1995; Wulfkuhle et al., 1998). Forked proteins have been localized to the developing bristles of *Drosophila* pupae by immunofluorescence (Petersen et al., 1994), suggesting that they, too, may be components of plasma membrane–associated parallel actin bundles. The forked proteins also appear to come in multiple isoforms: six *forked* transcripts have been detected during mid to late pupal development, and five of the six isoforms are predicted to share a COOH-terminal peptide, which includes the 66–amino acid peptide with 39% identity to the forked homology peptide present in the shared COOH-terminal peptide of the espins (Hoover et al., 1993; Bartles et al., 1996). On the basis of the ability of one of the smaller forked proteins to restore normal actin bundle and bristle morphology in transgenic *forked* mutant pupae, it is presumably the shared COOH-terminal peptide that contains the actin-bundling module postulated to exist within the forked proteins (Petersen et al., 1994). A peptide present within the shared COOH-terminal peptide of the forked proteins—the one encoded by exon A5 of the *forked* gene that includes the 66–amino acid peptide with homology to the espins—has, in fact, been observed to bind to F-actin (Petersen, N.S., personal communication). Although other primary structural features of the forked proteins (e.g., the alternating histidine and proline residues of the PRD-like domain, the polyglutamine tracts encoded by the CAX trinucleotide repeats, and the peptides composed of large numbers of predominantly hydrophobic amino acids) are notably absent from the espins, the larger isoforms of the forked proteins do contain two proline-rich peptides and NH_2-terminal ankyrin-like repeats with an overall spacing that approximates that observed in the large isoform of espin (Hoover et al., 1993; Bartles et al., 1996). It is presently unclear whether forked proteins will be found in other tissues of *Drosophila*. The *forked* phenotype appears to be limited to the neurosensory bristles of pupae and to the hairs and denticles of larvae and adults, and to our knowledge, these are the only structures in *Drosophila* found, or postulated, to contain a forked protein to date (Hoover et al., 1993; Petersen et al., 1994; Tilney et al., 1995; Dickinson and Thatcher, 1997; Wulfkuhle et al., 1998).

Toward a Three Actin-bundling Protein Model

At a minimum, our results suggest that microvillar actin bundles are even more complex and heterogeneous than thought previously. On the basis of our findings, we propose that in some cells it may take not two, but three actin-bundling proteins to construct and/or maintain a fully functional microvillar actin bundle. An extension of the prevailing two-bundling protein model (Tilney et al., 1995), the three-bundling protein model would appear to be consistent with the results of recent experiments examining pupal bristle formation in *singed/forked* double mutants of *Drosophila* that imply the involvement of at least one additional actin-bundling protein (Wulfkuhle et al., 1998). It would also appear to follow logically from our observation that small espin is present at different levels in the brush borders of cells that line different segments of the proximal tubule in rat kidney. In this regard, it may be relevant that the cells in the kidney we found to contain the largest amounts of brush border small espin, those lining the distal straight segment (S3) of the proximal tubule, are also known to display microvilli that are longer and more densely packed than those in other segments of the proximal tubule in the rat (Kriz and Kaissling, 1992).

Small espin appeared to be 10- to 20-fold less abundant than the two known major actin-bundling proteins, fimbrin/plastin and villin, in small intestinal brush borders isolated from adult rats. Barring losses due to degradation or extraction during brush border isolation, we can estimate that there is only ~1 espin for every 130 actin monomers present in the intestinal brush border. Whether calculated assuming the theoretical value for maximally cross-linked, hexagonally packed filaments of ~1 cross-link for every 4.3 actin monomers (Tilney et al., 1995), or calculated using the ~10:0.65:1.3 molar ratio of actin monomer/fimbrin/villin in isolated intestinal brush borders (Coluccio and Bretscher, 1989), this stoichiometry suggests that only ~1 in every 30 crossbridges between actin filaments would be due to small espin in the microvillar actin bundles of the adult small intestine. Although its lower abundance may help to explain why small espin escaped the attention of earlier investigators, it makes it more challenging for us to identify the role(s) of small espin in microvillar actin bundle organization and/or function.

Possible Roles for Small Espin as a High-affinity, Ca^{2+}-insensitive Cross-Linker, Filament Stabilizer, and/or Linker Protein

In the context of a three-bundling protein hypothesis, it is possible to envision at least a few different scenarios that would be compatible with the available evidence. One especially intriguing possibility is that small espin might confer a special property upon the bundle and that it is sufficient to have the cross-links involving this third bundling protein spaced relatively far apart in the completed structure. One obvious special property that small espin could confer upon a bundle is high-affinity cross-linking that is insensitive to changes in the concentration of Ca^{2+}. Small espin exhibits a binding affinity for F-actin that is at least an order of magnitude higher than those displayed by many of the other known actin-bundling proteins, including fimbrin/plastin and villin (Glenney et al., 1981; Burgess et al., 1987; Pollard, 1993). In addition, both villin and fimbrin/plastin have binding sites for Ca^{2+}, and the bundling activities of villin and fimbrin/plastin are known to be disrupted by physiological concentrations of Ca^{2+} (Glenney et al., 1981; Alicea and Mooseker, 1988; Namba et al., 1992; Lin et al., 1994). However, we found that the actin-bundling activity of small espin was insensitive to changes in the concentration of Ca^{2+} over a wide range. We are currently testing the hypothesis that strategic placement of

Published October 5, 1998

small espin at intervals along the filaments might reinforce the bundle by protecting it from changes in Ca^{2+} concentration.

A second special property that small espin might be able to confer upon actin bundles is stabilization to depolymerization. This would be one possible explanation for the apparent accumulation of F-actin we noted in the small espin-expressing transfected cells. A similar stabilization effect, apparently independent of cross-linking, has already been noted in vitro for one actin-bundling protein, the ~34-kD actin-bundling protein of *Dictyostelium* (Zigmond et al., 1992). In the case of the small espin-expressing transfected cells, it is difficult to sort out the effects of stabilization versus bundling. For example, we do not yet know the extent to which the F-actin fibers and cables observed in the transfected cells contain parallel actin bundles in addition to the antiparallel (contractile) bundles typical of stress fibers. We are currently carrying out experiments to determine whether the espin isoforms can stabilize F-actin independently of cross-linking. We are also investigating the possibility that the apparent accumulation of F-actin observed in the transfected cells reflects an increase in actin synthesis to maintain a sizable pool of monomer. Nevertheless, it is striking that the results we obtained with small espin are quite different from those obtained by others examining the localization and effects of villin and fimbrin/plastin in transfected fibroblastic cells: villin causes a loss of stress fibers and the redistribution of F-actin into long spike-like microvilli at the dorsal surface (Friederich et al., 1989), whereas T- and L-plastins cause fibroblastic cells to round up and reorganize their stress fibers into geodesic structures (Arpin et al., 1994). We are currently comparing the localizations and effects of the espin isoforms in transfected epithelial cells.

Another special property that could be conferred upon the bundles by small espin might be to link the bundles to other proteins, possibly even to those of signaling cascades. The ability to act as a linker or adaptor protein would appear to be especially likely for the large isoform of espin, with its multiple motifs for protein–protein interaction—the ankyrin repeats and the proline-rich peptides (for additional discussion, see Bartles et al., 1996)—but could also readily apply in the case of the small isoform. We are currently using a combination of affinity approaches and two-hybrid screens to identify espin-binding proteins other than actin.

Developmental Accumulation of Small Espin

One possible explanation for why small espin is relatively minor in the intestinal brush borders of adult rats is that it might be required at an earlier step in brush border assembly. In such a case, it might be expressed at lower levels or be more unstable in adults. The results of our immunoperoxidase localization of small espin in the small intestines of adult rats suggest, however, that this is probably not the case. In many respects, the assembly of the intestinal brush border along the crypt–villus axis in the adult approximates an accelerated version of intestinal brush border assembly during late embryonic development (Heintzelman and Mooseker, 1992; Fath and Burgess, 1995). We noted a large differential in the intensity of apical immunoperoxidase staining between crypt cells and villus cells in adult intestine. Although there are some limitations inherent in trying to use immunoperoxidase histochemistry as a quantitative measure, our results suggest that maximal small espin accumulation occurs not early, but relatively late during enterocyte differentiation and brush border assembly. In contrast, both villin and fimbrin/plastin have been found to be nearly as prevalent in the apical cytoplasm of crypt cells in the adult as they are in the brush borders of the mature enterocytes (Fath et al., 1990; Heintzelman and Mooseker, 1990; Landry et al., 1994). The increase in immunoperoxidase staining for small espin was first noted for enterocytes nearing the crypt–villus junction, roughly coinciding with the timing of the terminal elongation of microvilli and the arrival of brush border myosin I (Heintzelman and Mooseker, 1992; Fath and Burgess, 1995). To address this issue more fully, we are carrying out an analysis of small espin expression and localization in relation to other brush border proteins during the development of intestine and kidney and in cell culture models of enterocyte differentiation.

Partial Redundancy and the Presence of Espins in Other Actin Bundle-containing Structures

Even though small espin appears not to be as major as fimbrin/plastin or villin in the intestinal brush borders of adults, it is still possible that it is much more abundant in other F-actin–containing structures in the body. This situation would be somewhat analogous to that of ezrin, which is a minor protein relative to brush border myosin I in the intestinal brush border, but appears to supplant brush border myosin I as the major F-actin–membrane linker of placental microvilli (Bretscher et al., 1997). In such a case, small espin could be partially redundant in function in the intestinal brush border of normal adult rats and of primary importance only when one of the other actin-bundling proteins is impaired or missing. In this regard, it has been reported that mice that are missing villin due to targeted gene disruption have surprisingly normal looking intestinal brush borders (Pinson et al., 1998). In preliminary experiments, increased levels of brush border espin have been detected in villin gene knock-out mice by immunofluorescence and Western blotting (Ferrary, E., and S. Robine, personal communication). In addition, we have obtained preliminary evidence that espin isoforms are indeed more plentiful in other structures that contain parallel actin bundles (unpublished data). The further characterization of the espin isoforms found in these other locations is in progress.

We thank Dr. Mike Shaw (University of Pennsylvania, Philadelphia, PA) for advice about immunogold labeling of brush borders; Dr. Dan Kiehart (Duke University, Chapel Hill, NC) for advice about PHEM buffers and coiled coils; Maya Moody for help with sectioning, microscopy, and digital imaging; Dr. Rob Moir and Miri Yoon for advice about bacterial expression and GFP transfection systems; Dr. Kate Spiegel for help with the analytical ultracentrifuge; Dr. Brian Schoichet for help with the circular dichroism spectroscopy; Jodi Irwin for help with automated sequencing; Dr. Nancy Petersen (University of Wyoming, Laramie, WY) and Dr. Evelyne Ferrary and Dr. Sylvie Robine (Institut Curie, Paris, France) for granting us permission to discuss their results before publication; and Dr. Rex Chisholm for valuable discussions.

This work was supported by American Cancer Society research grant

#CB-203, National Institutes of Health (NIH) grant R01 HD35280, and NIH Independent Scientist Award K02 HD01210 awarded to J.R. Bartles.

Received for publication 14 July 1998 and in revised form 27 August 1998.

References

Alicea, H.A., and M.S. Mooseker. 1988. Characterization of villin from the intestinal brush border of the rat, and comparative analysis with avian villin. *Cell Motil. Cytoskel.* 9:60–72.

Altschul, S.F., W. Gish, W. Miller, E.W. Myers, and D.J. Lipman. 1990. Basic local alignment search tool. *J. Mol. Biol.* 215:403–410.

Arpin, M., E. Friederich, M. Algrain, F. Vernel, and D. Louvard. 1994. Functional differences between L- and T-plastin isoforms. *J. Cell Biol*. 127:1995–2008.

Bartles, J.R., A. Wierda, and L. Zheng. 1996. Identification and characterization of espin, an actin-binding protein localized to the F-actin-rich junctional plaques of Sertoli cell ectoplasmic specializations. *J. Cell Sci.* 109:1229–1239.

Berger, B., D.B. Wilson, E. Wolf, T. Tonher, M. Milla, and P.S. Kim. 1995. Predicting coiled coils by use of pairwise residue correlations. *Proc. Natl. Acad. Sci. USA*. 92:8259–8263.

Bretscher, A., D. Reczek, and M. Berryman. 1997. Ezrin: a protein requiring conformational activation to link microfilaments to the plasma membrane in the assembly of cell surface structures. *J. Cell Sci.* 110:3011–3018.

Burgess, D.R., K.O. Broschat, and J.M. Hayden. 1987. Tropomyosin distinguishes between the two actin-binding sites of villin and affects actin-binding properties of other brush border proteins. *J. Cell Biol.* 104:29–40.

Burridge, K., and M. Chrzanowska-Wodnicka. 1996. Focal adhesions, contractility and signaling. *Annu. Rev. Cell Dev. Biol.* 12:463–518.

Carlier, M.R. 1997. Control of actin dynamics. *Curr. Opin. Cell Biol*. 10:45–51.

Chen, Y.-H., J.T. Yang, and K.H. Chau. 1974. Determination of the helix and β forms of proteins in aqueous solution by circular dichroism. *Biochemistry*. 13:3350–3359.

Chou, P.Y., and G.D. Fasman. 1978. Prediction of the secondary structure of proteins from their amino acid sequence. *Adv. Enzymol. Relat. Areas Mol. Biol*. 47:45–148.

Coluccio, L.M., and A. Bretscher. 1989. Reassociation of microvillar core proteins: making a microvillar core in vitro. *J. Cell Biol.* 108:495–502.

Cooper, J.A., and T.D. Pollard. 1982. Methods to measure actin polymerization. *Methods Enzymol.* 85:182–210.

Devereux, J., P. Haeberli, and O. Smithies. 1984. A comprehensive set of sequence analysis programs for the VAX. *Nucleic Acids Res.* 12:387–395.

Dickinson, W.J., and J.W. Thatcher. 1997. Morphogenesis of denticles and hairs in *Drosophila* embryos: involvement of actin-associated proteins that also affect adult structures. *Cell Motil. Cytoskel.* 38:9–21.

Edwards, R.A., H. Herrera-Sosa, J. Otto, and J. Bryan. 1995. Cloning and expression of a murine fascin homolog from mouse brain. *J. Biol. Chem.* 270: 10764–10770.

Ezzell, R.M., M.M. Chafel, and P.T. Matsudaira. 1989. Differential localization of villin and fimbrin during development of the mouse visceral endoderm and intestinal epithelium. *Development (Camb.)*. 106:407–419.

Fath, K.R., and D.R. Burgess. 1995. Microvillus assembly: not actin alone. *Curr. Biol*. 5:591–593.

Fath, K.R., S.D. Obenauf, and D.R. Burgess. 1990. Cytoskeletal protein and mRNA accumulation during brush border formation in adult chicken enterocytes. *Development (Camb.)*. 109:449–459.

Friederich, E., C. Huet, M. Arpin, and D. Louvard. 1989. Villin induces microvilli growth and actin redistribution in transfected fibroblasts. *Cell*. 59: 461–475.

Friederich, E., E. Pringault, M. Arpin, and D. Louvard. 1990. From the structure to the function of villin, an actin-binding protein of the brush border. *Bioessays*. 12:403–408.

Furukawa, R., and M. Fechheimer. 1997. The structure, function, and assembly of actin filament bundles. *Int. Rev. Cytol.* 175:29–90.

Garnier, J., D.J. Osguthorpe, and B. Robson. 1978. Analysis of the accuracy and implications of simple methods for predicting the secondary structure of globular proteins. *J. Mol. Biol.* 120:97–120.

Glenney, J.R., Jr., P. Kaulfus, P. Matsudaira, and K. Weber. 1981. F-actin binding and bundling properties of fimbrin, a major cytoskeletal protein of microvillus core filaments. *J. Biol. Chem*. 256:9283–9288.

Goldsmith, S.C., N. Pokala, W. Shen, A.A. Federov, P. Matsudaira, and S.C. Almo. 1997. The structure of an actin-crosslinking domain from human fimbrin. *Nat. Struct. Biol.* 4:708–712.

Gumbiner, B.M. 1996. Cell adhesion: the molecular basis of tissue architecture and morphogenesis. *Cell*. 84:345–357.

Hall, A. 1998. Rho GTPases and the actin cytoskeleton. *Science*. 279:509–514.

Heintzelman, M.B., and M.S. Mooseker. 1990. Assembly of the brush border cytoskeleton: changes in the distribution of microvillar core proteins during enterocyte differentiation in adult chicken intestine. *Cell Motil. Cytoskel.* 15: 12–22.

Heintzelman, M.B., and M.S. Mooseker. 1992. Assembly of the intestinal brush border cytoskeleton. *Curr. Top. Dev. Biol.* 26:93–122.

Hoover, K.K., A.J. Chien, and V.G. Corces. 1993. Effect of transposable elements on the expression of the forked gene of *Drosophila melanogaster*. *Genetics*. 135:507–526.

Keller, T.C.S., III, and M.S. Mooseker. 1982. Ca^{++}-calmodulin–dependent phosphorylation of myosin, and its role in brush border contraction in vitro. *J. Cell Biol*. 95:943–959.

Kozak, M. 1987. An analysis of 5′-noncoding sequence from 699 vertebrate messenger RNAs. *Nucleic Acids Res*. 15:8125–8148.

Kriz, W., and B. Kaissling. 1992. Structural organization of the mammalian kidney. *In* The Kidney: Physiology and Pathophysiology, 2nd edition. D.W. Seldin and G. Giebisch, editors. Raven Press, New York. 707–777.

Landry, C., C. Huet, P. Mangeat, A. Sahuquet, D. Louvard, and P. Crine. 1994. Comparative analysis of neutral endopeptidase (NEP) and villin gene expression during mouse embryogenesis and enterocyte maturation. *Differentiation*. 56:55–65.

Lin, C.S., W. Shen, Z.P. Chen, Y.H. Tu, and P. Matsudaira. 1994. Identification of I-plastin, a human fimbrin isoform expressed in intestine and kidney. *Mol. Cell Biol*. 14:2457–2467.

Lupas, A. 1997. Predicting coiled-coil regions in proteins. *Curr. Opin. Struct. Biol*. 7:388–393.

Matsudaira, P. 1991. Modular organization of actin crosslinking proteins. *Trends Biochem. Sci.* 16:87–92.

McKnight, C.J., D.S. Doering, P.T. Matsudaira, and P.S. Kim. 1996. A thermostable 35-residue subdomain within villin headpiece. *J. Mol. Biol.* 260:126–134.

McKnight, C.J., P.T. Matsudaira, and P.S. Kim. 1997. NMR structure of the 35-residue villin headpiece subdomain. *Nat. Struct. Biol.* 4:180–184.

Mermall, V., P.L. Post, and M.S. Mooseker. 1998. Unconventional myosins in cell movement, membrane traffic, and signal transduction. *Science*. 279:527–533.

Mitchison, T.J., and L.P. Cramer. 1996. Actin-based motility and cell locomotion. *Cell*. 84:371–379.

Namba, Y., M. Ito, Y. Zu, K. Shigesada, and K. Maruyama. 1992. Human T cell L-plastin bundles actin filaments in a calcium-dependent manner. *J. Biochem.* 112:503–507.

Petersen, N.S., D.-H. Lankenau, H.K. Mitchell, P. Young, and V.G. Corces. 1994. Forked proteins are components of fiber bundles present in developing bristles of *Drosophila melanogaster*. *Genetics.* 136:173–182.

Pinson, K.I., L. Dunbar, L. Samuelson, and D.L. Gumucio. 1998. Targeted disruption of the mouse villin gene does not impair the morphogenesis of microvilli. *Dev. Dyn*. 211:109–121.

Pollard, T.D. 1993. Actin and actin-binding proteins. *In* Guidebook to the Cytoskeletal and Motor Proteins. T. Kreis and R. Vale, editors. Oxford University Press, Oxford. 3–11.

Puius, Y.A., N.M. Mahoney, and S.C. Almo. 1998. The modular structure of actin-regulatory proteins. *Curr. Opin. Cell Biol*. 10:23–34.

Ridley, A.J. 1995. Rho-related proteins: actin cytoskeleton and cell cycle. *Curr. Opin. Genet. Dev*. 5:24–30.

Rodman, J.S., M. Mooseker, and M.G. Farquhar. 1986. Cytoskeletal proteins of the rat proximal tubule brush border. *Eur. J. Cell Biol.* 42:319–327.

Russell, L.D., and R.N. Peterson. 1985. Sertoli cell junctions: morphological and functional correlates. *Int. Rev. Cytol*. 94:177–211.

Stokes, D.L., and D.J. DeRosier. 1991. Growth conditions control the size and order of actin bundles in vitro. *Biophys. J*. 59:456–465.

Su, J.Y., R.S. Hodges, and C.M. Kay. 1994. Effect of chain length on the formation and stability of synthetic α-helical coiled coils. *Biochemistry*. 33:15501–15510.

Tang, J.X., and P.A. Janmey. 1996. The polyelectrolyte nature of F-actin and the mechanism of actin bundle formation. *J. Biol. Chem*. 271:8556–8563.

Tilney, L.G., M.S. Tilney, and D.J. DeRosier. 1992. Actin filaments, stereocilia and hair cells: how cells count and measure. *Annu. Rev. Cell Biol.* 8:257–274.

Tilney, L.G., M.S. Tilney, and G.M. Guild. 1995. F-Actin bundles in *Drosophila* bristles. I. Two filament cross-links are involved in bundling. *J. Cell Biol.* 130:629–638.

Vogl, A.W. 1989. Distribution and function of organized concentrations of actin filaments in mammalian spermatogenic cells and Sertoli cell. *Int. Rev. Cytol.* 119:1–56.

Walsh, T.P., A. Weber, K. Davis, E. Bonder, and M. Mooseker. 1984. Calcium dependence of villin-induced actin depolymerization. *Biochemistry*. 23: 6099–6102.

Wulfkuhle, J.D., N.S. Petersen, and J.J. Otto. 1998. Changes in the F-actin cytoskeleton during neurosensory bristle development in *Drosophila*: the role of singed and forked proteins. *Cell Motil. Cytoskel*. 40:119–132.

Zhou, N.E., C.M. Kay, and R.S. Hodges. 1992. Synthetic model proteins. Positional effects of interchain hydrophobic interactions on stability of two-stranded α-helical coiled-coils. *J. Biol. Chem*. 267:2664–2670.

Zigmond, S.H., R. Furukawa, and M. Fechheimer. 1992. Inhibition of actin filament depolymerization by the *Dictyostelium* 30,000-D actin-bundling protein. *J. Cell Biol.* 119:559–567.